Optica Applicata, Vol. LI, No. 4, 2021
DOI: 10.37190/oa210401

Influence of optical Airy transform on non-diffracting propagation distance of finite energy Airy beams

XINGCHUN CHU*, RONGJIANG LIU, XIANG WANG, ZHONGXIANG HAN, YANHUI NI

Information and Navigation College, AFEU, Xi'an, 710077, China

*Corresponding author: kejdcxc@163.com

Finite energy Airy beams (FEAB) generated in laboratory have a short non-diffracting propagation distance (NDPD), which restricts its application in laser communication, laser detection and other fields. Effects of optical Airy transform (OAT) on NDPD of FEAB is analyzed. By comparing the theoretical formulas of the FEAB before and after the OAT, we find that when the transform parameter α of the OAT is larger than zero, the transverse scaling factor of the transformed FEAB is greater than that before the transformation, while the transformed exponential decay factor is smaller than that before the transformation. Using the Huygens–Fresnel diffractive integral, we derive the propagation formula of the transformed FEAB. Initial intensity distribution of FEAB before and after the OAT is compared. Propagation dynamics of the transformed FEAB with different α is numerically simulated and its NDPD is quantitatively evaluated. Results show that: with the increase of α, side lobes of the transformed FEAB increase, its main lobe and side lobes become wider than that before the transformation, and the inclination of the propagation trajectory decreases. When α is greater than half of the transverse scaling factor, the NDPD of the transformed FEAB increases rapidly.

Keywords: physics optics, non-diffracting beam, finite energy Airy beams, non-diffracting propagation distance, optical Airy transform.

1. Introduction

Free-space optical (FSO) communication is a promising communication technology for high-data-rate information transmission that is available at optical frequencies [1, 2]. For FSO links using Gaussian beam as an optical carrier, beam diffraction and atmospheric turbulence are the two main factors affecting its performance, especially when the propagation distance is more than 1 km [3, 4]. Therefore, it is a natural idea to improve the performance of FSO links by replacing the traditional Gaussian beam with a non-diffracting beam such as Airy beam or Bessel beam [5].

As a new type of non-diffracting beam, Airy beam is the solution of Helmholtz wave equation and can keep its transverse intensity distribution invariant in a long propagation distance [6–8]. it has attracted extensive attention due to its unique characteristics of non-diffracting, self-accelerating and self-healing [9–11]. Finite energy Airy beams (FEAB) has much longer non-diffracting propagation distance (NDPD) than the Rayleigh distance of traditional Gaussian beam and its scintillation index is also much smaller than that of Gaussian beam. These characteristics make FEAB have potential to suppress diffraction effect and atmospheric turbulence effect in laser communication and laser detection systems. Therefore, researchers have extensively studied the propagation and evolution of FEAB in atmospheric turbulence [12–15], far-field divergence [16, 17], scintillation behavior [18–20] and beam wander [21–23], *etc*., and applications of FEAB in optical route [24], image signal transmission [25], label-free imaging [8] and obstacle evasion in FSO links [26] have been reported. However, an important problem that has been selectively neglected in literatures is that the NDPD of FEAB generated in laboratories at present is very short, which can only transmit a few centimeters to a few meters without diffraction, and cannot be used in the fields of FSO communication requiring long-distance transmission. Therefore, how to extend the NDPD of FEAB is one of the key problems hindering its application.

In this paper, the influence of optical Airy transform (OAT) on the NDPD of FEAB is studied. Reference [27] gave the analytical expressions at the initial plane of the FEAB before and after the OAT, but did not analyze their propagation characteristics. Firstly, we compared the expressions at the initial plane of the FEAB before and after the OAT. We found that the OAT can increase the transverse scaling factor and reduce the exponential decay factor when the transform parameter α is greater than zero. Secondly, we developed the propagation dynamic formula of the transformed FEAB by using the Huygens–Fresnel diffractive integral. And numerical results show that the OAT can effectively extend the NDPD of the FEAB.

2. Theoretical model of OAT

Figure 1 shows the optical setup of the OAT [27–30]. The coordinates of input plane and output plane are $(x_\mathrm{i}, y_\mathrm{i})$ and $(x_\mathrm{o}, y_\mathrm{o})$, respectively. The directions of the x axis and y axis of the output plane are opposite to those of the input plane and the spatial light modulator (SLM) plane.

If 1D FEAB is transformed, the phase pattern applied to the SLM is [27, 30]

$$\Phi(x_\mathrm{s}) = \frac{\alpha k_x^3}{3} - (4kf + \pi) \tag{1}$$

where α is transform parameters of the OAT and real constant, $k = 2\pi/\lambda$ is the wave number, $k_x = kx_\mathrm{s}/f$, and f is the focal length of the lens.

The electric field of the FEAB at the input plane is [9, 11]

$$U_\mathrm{i}(x_\mathrm{i}) = \mathrm{Ai}\left(\frac{x_\mathrm{i}}{x_0}\right)\exp\left(\frac{a_0 x}{x_0}\right) \tag{2}$$

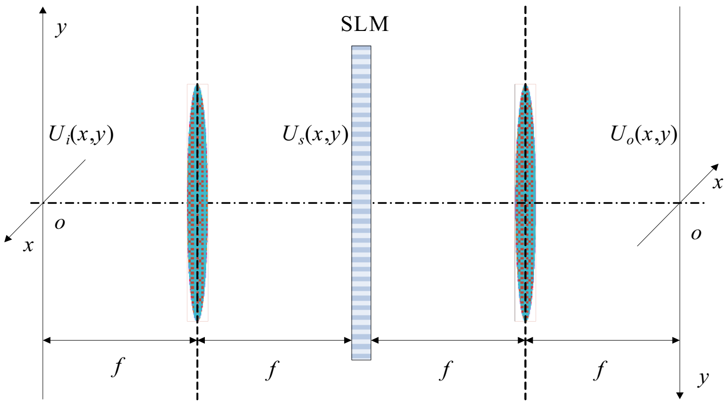

Fig. 1. The optical setup of Airy transform, f is the focal length of the lens, the SLM imposes the cubic phase modulation on the input light beams.

where Ai(·) is Airy function, x_0 is transverse scaling factor, a_0 is exponential decay factor. The FEAB becomes the 1D ideal Airy beam when $a_0 = 0$.

If $x_0 \neq -\alpha$, the electric field at the output plane of the OAT is [27]

$$U_o(x) = A_1 \operatorname{Ai}\left(\frac{x}{\gamma_x} - \frac{a_1^2 \alpha^3}{x_0^3}\right) \exp\left(\frac{a_1 x}{\gamma_x}\right) \tag{3}$$

where

$$\gamma_x^3 = \alpha^3 + x_0^3 \tag{3a}$$

$$a_1 = a_0 x_0^2 / \gamma_x^2 \tag{3b}$$

$$A_1 = \frac{x_0}{|\gamma_x|} \exp\left(-\frac{a_0^2 \alpha^3}{3\gamma_x^3}\right) \tag{3c}$$

Comparing Eqs. (2) and (3), we can see that an input FEAB is transformed into a new FEAB by the OAT [31]. The transverse scaling factor changes from x_0 to γ_x, and the exponential decay factor also changes from a_0 to a_1. Because of $x_0 > 0$, according to Eq. (3a), we can know the new transverse scaling factor γ_x which is greater than x_0 if the transform parameter $\alpha > 0$. According to Eq. (3b), the new exponential decay factor a_1 is smaller than a_0.

Figure 2 shows the curves of transverse scaling factor γ_x (**a**) and exponential decay factor a_1 (**b**) as a function of the transform parameter α. From Fig. 2**a**, we can see that γ_x increases almost linearly when α is greater than x_0. From Fig. 2**b**, it is clear that a_1 decreases rapidly within the range of $0 < \alpha < 2x_0$. As is known to all, if the transverse scaling factor of FEAB is increased or the exponential decay factor is decreased,

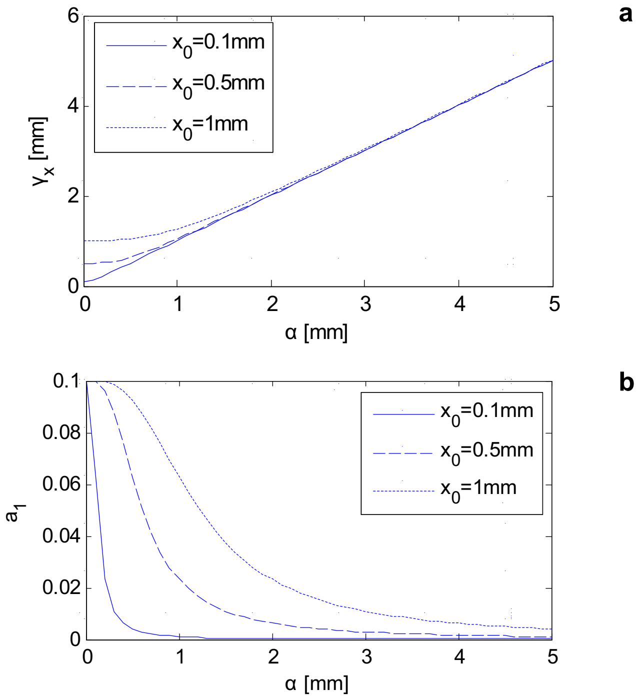

Fig. 2. The curves of γ_x and a_1 changing with parameter α of OAT and $a_0 = 0.1$. (**a**) γ_x as function of α, and (**b**) a_1 as function of α.

the NDPD of the FEAB would be extended [32]. Therefore, choosing a proper transform parameter α, the OAT may increase the NAPD of the FEAB.

3. Comparison of propagation dynamics of FEAB before and after the OAT

According to Eqs. (2) and (3), we can calculate the initial amplitude distribution of FEAB before and after the OAT, as shown in Fig. 3. The blue line represents the amplitude distribution before the transformation, and the red dash line represents the amplitude distribution after the transformation. The values of α in Figs. 3**a**–3**c** are 0.5, 1, and 2 mm, respectively. It can be seen that the peak amplitude of the transformed FEAB decreases with the increase of α, and its main lobe moves in the negative direction and widens. In addition, with the increase of α, the amplitude of the main lobe decreases while amplitudes of side lobes increase, and the trailing tail of the transformed FEAB becomes longer. This means that when the transform parameter α is positive, the OAT can extend the NDPD of the FEAB.

In order to analyze the propagation dynamics of the FEAB, we derive its analytical expression. Before the OAT, the field of the FEAB at the initial plane ($z = 0$) is described by Eq. (2). Its propagation field can be expressed as [10, 11]

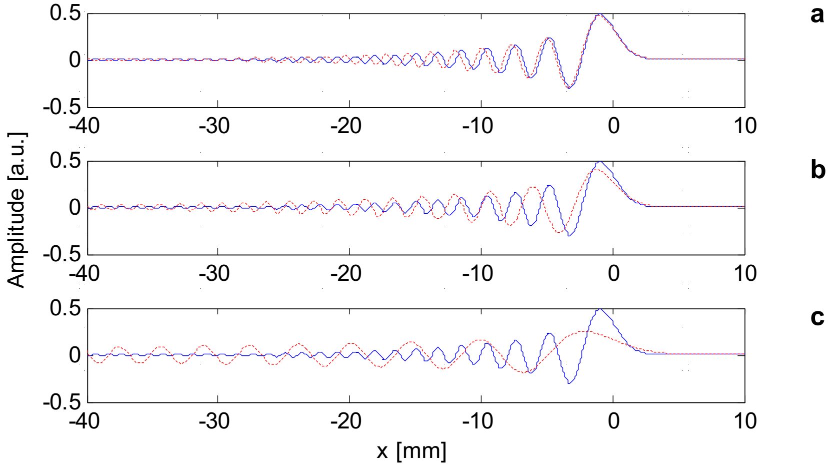

Fig. 3. The initial amplitude profile of FEAB before (blue line) and after (red dash line) the OAT as a function of x. The values of α are 0.5 mm (**a**), 1 mm (**b**), and 2 mm (**c**). The blue line is calculated from Eq. (2) and the red dash line from Eq. (3). The transvers scaling factor $x_0 = 1$ mm and exponential decay factor $a_0 = 0.1$, the wavelength $\lambda = 1555$ nm,

$$U_{\mathrm{before}}(x, z) = \mathrm{Ai}\left(\frac{x}{x_0} - \left(\frac{z}{2kx_0^2}\right)^2 + ia_0\frac{z}{kx_0^2}\right) \times \exp\left(\frac{a_0 x}{x_0} - \frac{a_0}{2}\left(\frac{z}{kx_0^2}\right)^2 - \frac{i}{12}\left(\frac{z}{kx_0^2}\right)^3 + \frac{ia_0^2}{2}\frac{z}{kx_0^2} + \frac{i}{2}\frac{x}{x_0}\frac{z}{kx_0^2}\right) \tag{4}$$

After the OAT, the field of the transformed FEAB at the initial plane ($z = 0$) is described by Eq. (3). Using Huygens–Fresnel diffractive integral, its propagation field can be deduced as follow [33]

$$U_{\mathrm{after}}(x, z) = \sqrt{\frac{i}{\lambda z}}\int U(x_1, z=0)\exp\left(-i\frac{k}{2z}(x^2 - 2xx_1 + x_1^2)\right)\mathrm{d}x_1$$

$$= \sqrt{\frac{i}{\lambda z}}\int A_{1x}\mathrm{Ai}\left(\frac{x_1}{\gamma_x} - \frac{a_1^2\alpha^3}{x_0^3}\right)\exp\left(\frac{a_1 x_1}{\gamma_x}\right) \times \exp\left(-i\frac{k}{2z}(x^2 - 2xx_1 + x_1^2)\right)\mathrm{d}x_1 =$$

$$= U_{\text{after}}(x,z) = A_{1x}\,\mathrm{Ai}\left(\frac{x}{\gamma_x} - \left(\frac{z}{2k\gamma_x^2}\right)^2 + ia_1\frac{z}{k\gamma_x^2} - \frac{a_1^2\alpha^3}{x_0^3}\right)$$
$$\times \exp\left(\frac{a_1 x}{\gamma_x} - \frac{a_1}{2}\left(\frac{z}{k\gamma_x^2}\right)^2 - \frac{i}{12}\left(\frac{z}{k\gamma_x^2}\right)^3 + i\frac{a_1^2}{2}\frac{z}{k\gamma_x^2}\right.$$
$$\left. + \frac{i}{2}\frac{x}{\gamma_x}\frac{z}{k\gamma_x^2} + i\frac{a_1^2\alpha^3}{2x_0^3}\frac{z}{k\gamma_x^2}\right) \tag{5}$$

where

$$A_{1x} = \frac{x_0}{|\gamma_x|}\exp\left(-\frac{a_0^2\alpha^3}{3\gamma_x^3}\right) \tag{5a}$$

From Eq. (5), it can be seen that the accelerated trajectory of the transformed FEAB is

$$\frac{x}{\gamma_x} = \left(\frac{z}{2k\gamma_x^2}\right)^2 + \frac{a_1^2\alpha^3}{x_0^3} \tag{6}$$

According to Eq. (4), the acceleration trajectory of the FEAB before the OAT is

$$\frac{x}{x_0} = \left(\frac{z}{2kx_0^2}\right)^2 \tag{7}$$

If the transform parameter α is zero, Eq. (5) degenerates into Eq. (4), and Eq. (6) is also reduced to Eq. (7). According to Eq. (5), we can analyze the influence of the OAT on the NDPD of the FEAB.

Figure 4 shows the propagation dynamics of the transformed FEAB with different transform parameter α. It can be seen that: with the increase of α, the number of side lobes of the transformed FEAB increases, the inclination of its propagation trajectory decreases, and the NDPD also extends significantly.

The NDPD is defined as the distance where the peak magnitude of main lobe of a beam at certain propagation distance drops below the –3 dB point of that at an initial plane. According to Eq. (5), the NDPD of the transformed FEAB can be numerically evaluated. Figure 5 shows the curve of the NDPD of the transformed FEAB as a function of the transform parameter α. The input transverse scaling factor $x_0 = 1$ mm, the exponential decay factor $a_0 = 0.1$, and the light wavelength $\lambda = 1555$ nm. When $\alpha = 0$, it means no OAT for the input FEAB, and its NDPD is about 16.7 m. When α is less

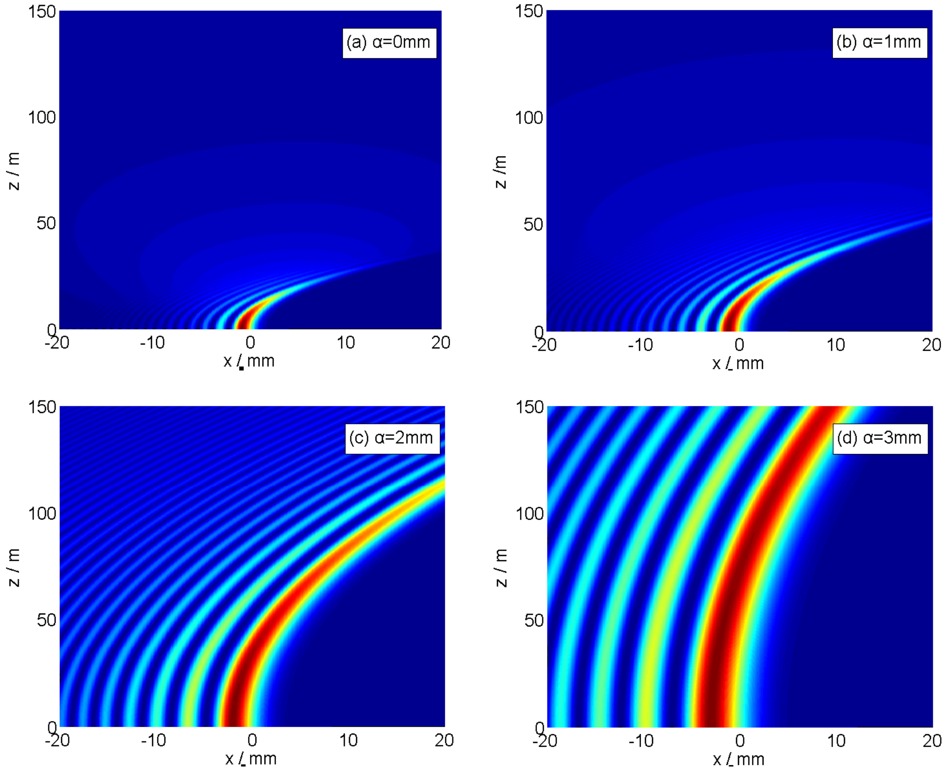

Fig. 4. Propagation dynamics of the transformed FEAB with different transform parameter α. The values of α are 0 (**a**), 1 mm (**b**), 2 mm (**c**), and 3 mm (**d**). The transverse scaling factor x_0 = 1 mm and the exponential decay factor a_0 = 0.1, the wavelength λ = 1555 nm.

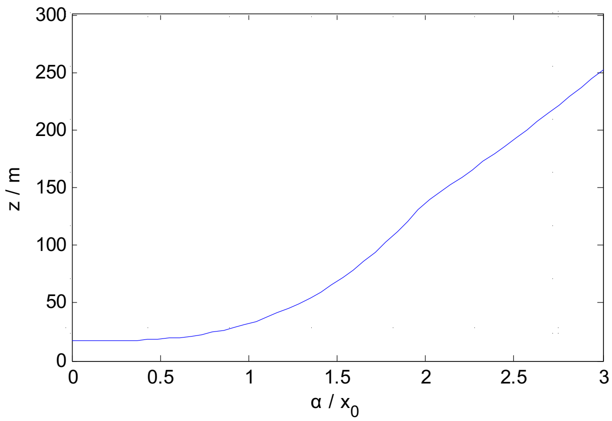

Fig. 5. NDPD of the transformed FEAB as a function of transform parameter α. Transverse scaling factor x_0 = 1 mm and exponential decay factor a_0 = 0.1, the wavelength λ = 1555 nm.

than $0.5x_0$, the NDPD of the transformed FEAB is less affected because the new transverse scaling factor γ_x in Eq. (3a) and the new exponential decay factor a_1 in Eq. (3b) change a little. And the NDPD of the transformed FEAB is almost the same as that of the input FEAB. When α is greater than $0.5x_0$, the NDPD of the transformed FEAB increases rapidly with the increase of α. When $\alpha = 3x_0$, the NDPD of the transformed FEAB extends to 250.6 m, which is much larger than the NDPD od the input FEAB. Figure 5 shows that the OAT can effectively extend the NDPD of FEAB by selecting proper transform parameter. This may expand the potential applications of the FEAB.

4. Conclusion

In this paper, the influence of OAT on the NDPD of the FEAB is analyzed. When the transform parameter is positive, the transverse scaling factor of the transformed FEAB becomes bigger than that of the input FEAB, and the exponential decay factor of the transformed FEAB changes less than that of the input FEAB. Based on Huygens –Fresnel diffractive integral, we derive the propagation dynamic formula of the transformed FEAB. The simulation results show that with the increase of the transform parameter, the peak amplitude of the transformed FEAB decreases, and its main lobe moves to the negative direction and widens. The amplitude and the number of side lobes increase. The inclination of the propagation trajectory of the transformed FEAB decreases. The OAT can effectively extend the NDPD of the FEAB by selecting proper transform parameter. Therefore, potential applications of the FEAB can be expanded.

Acknowledgment – This work was supported by the Shaanxi Provincial Natural Science Foundation of China (grant number 2019JM-176).

References

[1] CHAABAN A., MORVAN J.M., ALOUINI M.S., *Free-space optical communications: capacity bounds, approximations, and a new sphere-packing perspective*, IEEE Transactions on communications **64**(3), 2016, pp. 1176–1191, DOI: 10.1109/TCOMM.2016.2524569.

[2] SUN X.L., DJORDJEVEC I.B., *Physical-layer security in orbital angular momentum multiplexing free -space optical communications*, IEEE Photonics Journal **8**(1), 2016, article 7901110, DOI: 10.1109/JPHOT.2016.2519279.

[3] BOSU R., PRINCE S., *Mitigation of turbulence induced scintillation using concave mirror in reflection -assisted OOK free space optical links*, Optics Communications **432**, 2019, pp. 101–111, DOI: 10.1016/j.optcom.2018.09.061.

[4] MAHDIEH M.H., POURNOURY M., *Atmospheric turbulence and numerical evaluation of bit error rate (BER) in free-space communication*, Optics & Laser Technology **42**(1), 2010, pp. 55–60, DOI: 10.1016/j.optlastec.2009.04.017.

[5] CHU X.C., ZHAO S.H., CHEN Z., LI Y.J., LI R.X., FANG Y.W., *Research progress of Airy beam and feasibility analysis for its application in FSO system*, Chinese Science Bulletin **61**(17), 2016, pp. 1963 –1974 (in Chinese), DOI: 10.1360/N972015-00265.

[6] ZHAN K.Y., ZHANG W.Q., JIAO R.Y., DOU L.C., LIU B., *Propagations of Airy beams with quadratic phase modulation, and their interaction in paraxial optical systems*, Optics Communications **474**, 2020, p. 126156, DOI: 10.1016/j.optcom.2020.126156.

[7] Zhu Y.F., Geng T., *Generation of high-quality circular Airy beams in laser resonator*, Acta Physica Sinica – Chinese Edition **69**(1), 2020, article 014205 (in Chinese), DOI: 10.7498/aps.69.20191088.
[8] Nagar H., Dekel E., Kasimov D., Roichman Y., *Non-diffracting beams for label-free imaging through turbid media*, Optics Letters **43**(2), 2018, pp. 190–193, DOI: 10.1364/OL.43.000190.
[9] Siviloglou G.A., Broky J., Dogariu A., Christodoulides D.N., *Ballistic dynamics of Airy beams*, Optics Letters **33**(3), 2008, pp. 207–209, DOI: 10.1364/OL.33.000207.
[10] Siviloglou G.A., Broky J., Dogariu A., Christodoulides D.N., *Observation of accelerating Airy beams*, Physical Review Letters **99**(21), 2007, article 213901, DOI: 10.1103/PhysRevLett.99.213901.
[11] Siviloglou G.A., Christodoulides D.N., *Accelerating finite energy Airy beams*, Optics Letters **32**(8), 2007, pp. 979–981, DOI: 10.1364/OL.32.000979.
[12] Chu X.X., *Evolution of an Airy beam in turbulence*, Optics Letters **36**(14), 2011, pp. 2701–2703, DOI: 10.1364/OL.36.002701.
[13] Ji X.L., Eyyuboglu H.T., Ji G.M., Jia X.H., *Propagation of an Airy beam through the atmosphere*, Optics Express **21**(2), 2013, pp. 2154–2164, DOI: 10.1364/OE.21.002154.
[14] Chen C.Y., Yang H.M., Kavehrad M., Zhou Z., *Propagation of radial Airy array beams through atmospheric turbulence*, Optics and Lasers in Engineering **52**, 2014, pp. 106–114, DOI: 10.1016/j.optlaseng.2013.07.003.
[15] Wen W, Chu X.X., Ma H.T., *The propagation of a combining Airy beam in turbulence*, Optics Communications **336**, 2015, pp. 326–329, DOI: 10.1016/j.optcom.2014.10.006.
[16] Xu Y.Q., Zhou G.Q., *The far-field divergent properties of an Airy beam*, Optics & Laser Technology **44**(5), 2012, pp. 1318–1323, DOI: 10.1016/j.optlastec.2011.12.037.
[17] Tao R.M., Si L., Ma Y.X., Zhou P., Liu Z.J., *Average spreading of finite energy Airy beams in non -Kolmogorov turbulence*, Optics and Lasers in Engineering **51**(4), 2013, pp. 488–492, DOI: 10.1016/j.optlaseng.2012.10.014.
[18] Gu Y., Gbur G., *Scintillation of Airy beam arrays in atmospheric turbulence*, Optics Letters **35**(20), 2010, pp. 3456–3458, DOI: 10.1364/OL.35.003456.
[19] Eyyuboglu H.T., *Scintillation behavior of Airy beam*, Optics & Laser Technology **47**, 2013, pp. 232 –236, DOI: 10.1016/j.optlastec.2012.08.029.
[20] Lu Q., Gao S.J., Shng L., Wu J.B., Qiao Y.F., *Generation of coherent and incoherent Airy beam arrays and experimental comparisons of their scintillation characteristics in atmospheric turbulence*, Applied Optics **56**(13), 2017, pp. 3750–3757, DOI: 10.1364/AO.56.003750.
[21] Wen W., Chu X.X., *Beam wander of partially coherent Airy beams*, Journal of Modern Optics **61**(5), 2014, pp. 379–384, DOI: 10.1080/09500340.2014.887154.
[22] Wen W., Chu X.X., Cai Y.J., *Dependence of the beam wander of an airy beam on its kurtosis parameter in a turbulent atmosphere*, Optics & Laser Technology **68**, 2015, pp. 6–10, DOI: 10.1016/j.optlastec.2014.10.020.
[23] Wen W., Jin Y., Hu M.J., Liu X.L., Cai Y.J., Zou C.J., Luo M., Zhou L.W., Chu X.X., *Beam wander of coherent and partially coherent Airy beam arrays in a turbulent atmosphere*, Optics Communications **415**, 2018, pp. 48–55, DOI: 10.1016/j.optcom.2018.01.033.
[24] Rose P., Diebel F., Boguslawski M., Denz C., *Airy beam induced optical routing*, Applied Physics Letters **102**(10), 2013, article 101101, DOI: 10.1063/1.4793668.
[25] Liang Y., Hu Y., Song D.H., Lou C.B., Zhang X.Z., Chen Z.G., Xu J.J., *Image signal transmission with Airy beams*, Optics Letters **40**(23), 2015, pp. 5686–5689, DOI: 10.1364/OL.40.005686.
[26] Zhu G.X., Wen Y.H., Wu X., Chen Y.J., Liu J., Yu S.Y., *Obstacle evasion in free-space optical communications utilizing Airy beams*, Optics Letters **43**(6), 2018, pp. 1203–1206, DOI: 10.1364/OL.43.001203.
[27] Jiang Y.F., Huang K.K., Lu X.H., *The optical Airy transform and its application in generating and controlling the Airy beam*, Optics Communications **285**(24), 2012, pp. 4840–4843, DOI: 10.1016/j.optcom.2012.08.003.

[28] YAALOU M., HRICHA Z., BELAFHAL A., *Propagation properties of finite cosh-Airy beams through an Airy transform optical system*, Optical and Quantum Electronics **51**, 2019, article 356, DOI: 10.1007/s11082-019-2075-6.
[29] YAALOU M., HRICHA Z., EL HALBA E.M., BELAFHAL A., *Production of Airy-related beams by an Airy transform optical system*, Optical and Quantum Electronics **51**, 2019, article 308, DOI: 10.1007/s11082-019-2023-5.
[30] EZ-ZARIY L., BOUFALAH F., DALIL-ESSAKALI L., BELAFHAL A., *Conversion of the hyperbolic-cosine Gaussian beam to a novel finite Airy-related beam using an optical Airy transform system*, Optik **171**, 2018, pp. 501–506, DOI: 10.1016/j.ijleo.2018.06.091.
[31] LIU H.L., LÜ Y.F., XIA J., PU X.Y., ZHANG L., *Generation and propagation dynamics of Airy beam with the tunable tail*, Journal of Modern Optics **63**(9), 2016, pp. 887–895, DOI: 10.1080/09500340.2015.1108469.
[32] CHU X.C., ZHAO S.H., FANG Y.W., *Maximum non-diffracting propagation distance of aperture-truncated Airy beams*, Optics Communications **414**, 2018, pp. 5–9, DOI: 10.1016/j.optcom.2018.01.001.
[33] MORRIES J. E., MAZILU M., BAUMGARTL J., CIZMAR T., DHOLAKIA K., *Propagation characteristics of Airy beams: dependence upon spatial coherence and wavelength*, Optics Express **17**(15), 2009, pp. 13236–13245, DOI: 10.1364/OE.17.013236.

Received April 30, 2020
in revised form September 9, 2020